THE JOURNAL OF BIOLOGICAL CHEMISTRY VOL. 289, NO. 47, pp. 32488–32498, November 21, 2014


# Structural Re-arrangement and Peroxidase Activation of Cytochrome *c* by Anionic Analogues of Vitamin E, Tocopherol Succinate and Tocopherol Phosphate*

Received for publication, July 31, 2014, and in revised form, September 22, 2014 Published, JBC Papers in Press, October 2, 2014, DOI 10.1074/jbc.M114.601377

**Naveena Yanamala[‡§1], Alexander A. Kapralov[‡§1], Mirjana Djukic[‡§1], Jim Peterson[§], Gaowei Mao[‡§], Judith Klein-Seetharaman[¶], Detcho A. Stoyanovsky[‡§], Jan Stursa[‖], Jiri Neuzil[**‡‡], and Valerian E. Kagan[‡§ §§¶¶‖‖2]**

*From the [‡]Center for Free Radical and Antioxidant Health, the Departments of [§]Environmental and Occupational Health, [§§]Pharmacology and Chemical Biology, [¶¶]Radiation Oncology, and [‖‖]Chemistry, University of Pittsburgh, Pittsburgh, Pennsylvania 15260, the [¶]Division of Metabolic and Vascular Health, Medical School, University of Warwick, Coventry CV4 7AL, United Kingdom, the [‖]Biomedical Research Center, University Hospital, Hradec Kralove 569810, Czech Republic, the **Institute of Biotechnology, Academy of Sciences of the Czech Republic, Prague 14220, Czech Republic, and the [‡‡]School of Medical Science, Griffith University, Southport, Queensland 4222, Australia*

**Background:** An anionic phospholipid, cardiolipin, converts cytochrome c into a peroxidase.
**Results:** Anionic tocopherol derivatives, tocopherol succinate and tocopherol phosphate, similarly to cardiolipin, unfold cytpchrome *c* and stimulate its peroxidase activity.
**Conclusion:** Peroxidase activation of cytochrome c by tocopherol analogues is one of their pharmacological mechanisms.
**Significance:** Peroxidase activation of cytochrome c may induce apoptosis and contribute to anti-cancer properties of α-tocopherol succinate.

**Cytochrome c is a multifunctional hemoprotein in the mitochondrial intermembrane space whereby its participation in electron shuttling between respiratory complexes III and IV is alternative to its role in apoptosis as a peroxidase activated by interaction with cardiolipin (CL), and resulting in selective CL peroxidation. The switch from electron transfer to peroxidase function requires partial unfolding of the protein upon binding of CL, whose specific features combine negative charges of the two phosphate groups with four hydrophobic fatty acid residues. Assuming that other endogenous small molecule ligands with a hydrophobic chain and a negatively charged functionality may activate cytochrome *c* into a peroxidase, we investigated two hydrophobic anionic analogues of vitamin E, α-tocopherol succinate (α-TOS) and α-tocopherol phosphate (α-TOP), as potential inducers of peroxidase activity of cytochrome *c*. NMR studies and computational modeling indicate that they interact with cytochrome *c* at similar sites previously proposed for CL. Absorption spectroscopy showed that both analogues effectively disrupt the Fe-S(Met$^{80}$) bond associated with unfolding of cytochrome *c*. We found that α-TOS and α-TOP stimulate peroxidase activity of cytochrome *c*. Enhanced peroxidase activity was also observed in isolated rat liver mitochondria incubated with α-TOS and tBOOH. A mitochondria-targeted derivative of TOS, triphenylphosphonium-TOS (mito-VES), was more efficient in inducing $H_2O_2$-dependent apoptosis in mouse embryonic cytochrome $c^{+/+}$ cells than in cytochrome $c^{-/-}$ cells. Essential for execution of the apoptotic program peroxidase activation of cytochrome *c* by α-TOS may contribute to its known anti-cancer pharmacological activity.**

From the time of vitamin E discovery nearly a century ago by the pioneers in nutrition research at the University of California at Berkeley (1), the mechanisms of its action have been mainly associated with the antioxidant function (2) and protection against adverse effects of rancid fats as it was required to prevent fetal resorption in pregnant, vitamin E-deficient rats fed readily oxidizable lard-containing diets. Based on myriads of research papers describing details of action of eight natural isoforms of vitamin E as sacrificial chain-breaking lipid radical scavengers in biomembranes and lipoproteins (3, 4), a plethora of preclinical studies and clinical trials have been conducted with the goal to minimize free radical damage associated with specific diseases and lifestyle patterns, including cancer, cardiovascular disorders, neurological impairments, strenuous exercise, aging, and environmental pollution. Despite optimistic expectations, the results of clinical intervention trials of vitamin E, alone or in combination with other antioxidants, and their subsequent meta-analysis did not reveal significant beneficial therapeutic or preventive effects (5–7). Although issues of bioavailability and optimized regimens may explain, at least in part, disappointments in the clinical potential of vitamin E, another possible reason is that the initial concept of its major role as a free radical scavenger needs further refinement. This has lead to new concepts regarding vitamin E properties independent of its antioxidant, radical-scavenging ability, particularly as a signaling molecule and structural stabilizer of

* This work was supported, in whole or in part, by National Institutes of Health Grants HL114453, U19 AIO68021, ES 020693, and ES 021068, by National Institute for Occupational Safety and Health Grant OH008282, and by Human Frontier Science Program Grant HFSP-RGP0013/2014.
[1] These authors contributed equally to this work.
[2] Supported in part by the Australian Research Council.
[3] To whom correspondence should be addressed: Center for Free Radical and Antioxidant Health, Dept. of Environmental and Occupational Health, University of Pittsburgh, Bridgeside Point 100 Technology Drive, Suite 350, Pittsburgh, PA 15219. Tel.: 412-624-9479; Fax: 412-624-9361; E-mail: kagan@pitt.edu.

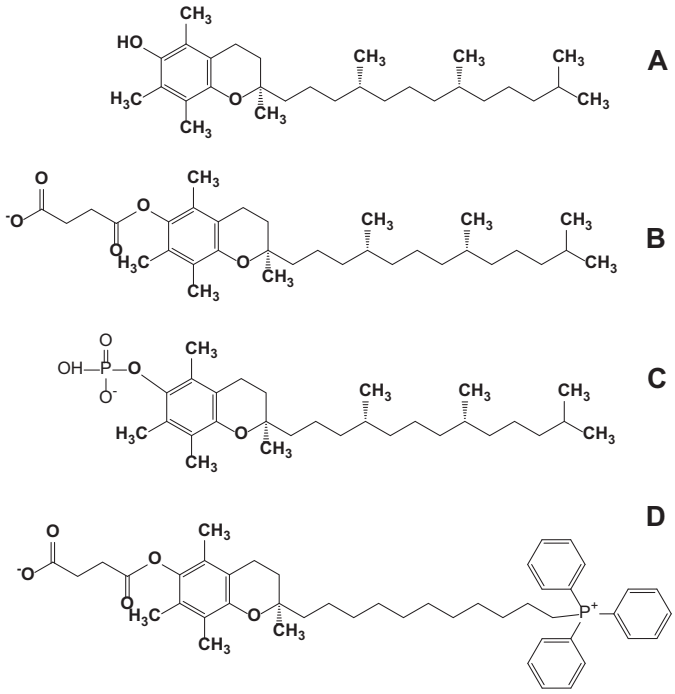


FIGURE 1. **Structural formulas of α-tocopherol (*A*), α-tocopherol succinate (*B*), α-tocopherol phosphate (*C*), and mito-VES (*D*).**

biomembranes (8, 9). At present, the physiological function(s) of vitamin E still remain largely unclear (10).

Recently, new pharmacological activities of tocopherol (TOC)[3] analogues, α-tocopherol succinate (α-TOS) and α-tocopherol phosphate (α-TOP) (Fig. 1), unrelated to the antioxidant activity, have been discovered in their applications as cardiovascular protectors and anti-cancer agents (11–15). The anti-tumor potential of α-TOS was linked to its ability to stimulate production of reactive oxygen species by targeting mitochondrial complex II, thus triggering pro-apoptotic cascades in cancer cells. Inhibitors of succinate:quinone reductase activity of complex II promote production of mitochondrial reactive oxygen species and protect normal cells from ischemic damage but induce specific cancer cell death (16). Accordingly, targeting of α-TOS into mitochondria by means of mitochondrially targeted vitamin E succinate (mito-VES, Fig. 1) via its conjugation with a cationic triphenylphosphonium group, enhanced the anti-tumor efficacy of the drug (17).

Execution of the apoptotic program includes the role of reactive oxygen species in selective peroxidation of a mitochondria-specific phospholipid, cardiolipin (CL) a process catalyzed by an intermembrane space hemoprotein, cytochrome *c* (18, 19). The emergence of peroxidase catalytic competence of cytochrome *c* is associated with partial unfolding of the protein that paves the way for the interaction of hydrogen peroxide (and organic hydroperoxides) with the penta-coordinated heme at the catalytic site of the protein (20). Structural analysis revealed the requirements sufficient for the fulfillment of the "unfolding task" by anionic phospholipid molecules: a combination of a negative charge(s), for the interaction with positively charged (Lys) residues on cytochrome *c* surface, with a hydrophobic moiety, for accessing the catalytic site through the hydrophobic pocket in the cytochrome *c* molecule (20, 21). Accordingly, several anionic phospholipids, phosphatidylserine (PS), phosphatidic acid, phosphatidylglycerol, and phosphatidylinositols, have been identified as activators, although not as strong as CL, of the dormant peroxidase function of cytochrome *c*. Given that molecules of α-TOS and α-TOP contain the requisite propensities and given their reported pro-apoptotic potential, in this study we explored the ability of the two derivatives of vitamin E to induce structural re-arrangements and unfold cytochrome *c*, thus "awakening" its peroxidase activity and enhancing apoptosis.

## EXPERIMENTAL PROCEDURES

*Materials*—Horse heart cytochrome *c* (type C-7752, >95%), diethylenetriaminepentaacetic acid (DTPA), D-α-tocopherol succinate, (±)-α-tocopherol phosphate disodium salt, $^{15}N$ isotope-labeled ammonium chloride ($NH_4Cl$), $H_2O_2$, and cholesterol were purchased from Sigma. 1,2-Dioleoyl-*sn*-glycero-3-phosphocholine (DOPC), 1,1′,2,2′-tetraoleoyl cardiolipin (TOCL), 1,2-dioleoyl-*sn*-glycero-3-phosphoethanolamine (DOPE), and sphingomyelin from porcine brain were obtained from Avanti Polar Lipids (Alabaster, AL). $^{13}S$-Hydroperoxy-9*Z*,11*E*-octadecadienoic acid ($^{13}S$-HpODE) was from Cayman Chemical (Ann Arbor, MI). Mito-VES has been synthesized and characterized as previously described (17). LB medium and Silver SNAP stain kit were purchased from Thermo Fisher Scientific (Rockford, IL). The CM-Sepharose fast flow column was from Amersham Biosciences, Inc.. Amplex Red (*N*-acetyl-3,7-dihydroxyphenoxazine) reagent was obtained from Molecular Probes (Eugene, OR). Amicon Ultra® 3K filters were obtained from EMD Millipore (Billerica, MA). The plasmid pJRhrsN2 was kindly provided by Dr. Jon Rumbley, Chemistry Department, University of Minnesota (Duluth, MN).

*Expression and Purification of $^{15}N$-Labeled Horse Heart Cytochrome c*—The competent cells, strain C41 (DE3) SOLOs (Lucigen® Corp.), were transformed with the plasmid, pJRhrsN2 (22), containing the recombinant pseudo-WT (pWT) cytochrome *c* gene carrying two mutations, H26N and H33N associated with the higher expression yields in *Escherichia coli* (23). Despite the mutations introduced, the pWT cytochrome *c* is structurally similar to WT cytochrome *c* (22, 23) and is a widely used as a model system (24–26). Cytochrome *c* was expressed and purified as described previously (22). Briefly, $^{15}N$-labeled pWT cytochrome *c* was expressed in *E. coli* by growing them in M9 minimal media containing $^{15}N$-labeled $NH_4Cl$. The expressed cytochrome *c* was purified using a CM-Sepharose fast flow column (22, 23). Fractions with a 410/280 nm absorbance ratio >4.0 were collected, and their purity was checked by SDS-PAGE using Coomassie Blue staining and silver staining. Following this, the fractions containing pure cytochrome *c* were spooled and concentrated (~2.8 mM) using an Amicon Ultra® 3K filter. Thus prepared stocks were further aliquoted,

[3] The abbreviations used are: TOC, tocopherol; TOS, α-tocopherol succinate; TOP, α-tocopherol phosphate; CL, cardiolipin; DTPA, diethylenetriaminepentaacetic acid; TOCL, 1,1′,2,2′-tetraoleoyl cardiolipin; DOPC, 1,2-dioleoyl-*sn*-glycero-3-phosphocholine; DOPE, 1,2-dioleoyl-*sn*-glycero-3-phosphoethanolamine; FFA-OOH, $^{13}S$-hydroperoxy-9*Z*,11*E*-octadecadienoic acid; mito-VES, triphenylphosphonium-TOS; PS, phosphatidylserine; HSQC, heteronuclear single quantum coherence; PE, phosphatidylethanolamine; PDB, Protein Data Bank.

snap frozen in liquid $N_2$ and stored at −80 °C for NMR measurements.

*Small Unilamellar Liposomes*—Liposomes were prepared from DOPC and TOCL (1:1 ratio) by sonication in 20 mM HEPES buffer (pH 7.4) with 100 μM DTPA.

*Isolation of Mitochondria*—The mitochondrial fraction was isolated from freshly obtained livers of adult male mice using differential centrifugation according to Ref. 27. The preparation was carried out in MSH buffer (210 mM mannitol, 70 mM sucrose, 5 mM HEPES, 1 mM EDTA, pH 7.5).

*NMR Spectroscopy*—$^{1}$H-$^{15}$N HSQC NMR spectra of uniformly $^{15}$N isotope-labeled cytochrome *c* were obtained using a ~900 MHz Bruker spectrometer. Two-dimensional $^{1}$H-$^{15}$N HSQC spectra of cytochrome *c* were acquired using a standard HSQC pulse sequence with 64 scans in the first dimension and 160 scans in the second dimension and a D1 delay of 1 s. Data acquisition was carried out using Topspin version 3.0 software (Bruker BioSpin Corp., Billerica, MA). Spectra were further processed and analyzed using NMRView (28) and Sparky (29). The HSQC NMR spectra of cytochrome *c* in the absence and presence of TOC analogues, α-TOS (50, 100, 150, and 200 μM) and α-TOP (50 and 100 μM), were acquired using a 50 μM purified $^{15}$N-labeled cytochrome *c* dissolved in 25 mM HEPES buffer (pH 7.4) and 10% $D_2O$. The backbone resonances observed in $^{1}$H-$^{15}$N HSQC spectra of pWT cytochrome *c* (22) were assigned using previously published NMR data, acquired under similar conditions (23).

*Computational Modeling Studies*—Three-dimensional structures of α-TOP and α-TOS were docked to the crystal structure of native cytochrome *c* (PDB code 1OCD) using AutoDock Vina (30). The presence of rotatable bonds imparted flexibility to the ligands. The structure of cytochrome *c* was considered to be rigid for docking. The grid box was centered at coordinates 0.244, 0.102, and −0.178 with 45-Å units in *x*, *y*, and *z* directions. This grid box covered the entire cytochrome *c* structure making the docking unbiased for different binding sites. The resulting orientations (a total of 9) in which the negative charged groups of α-TOP/α-TOS are in close proximity to positively charged residues on cytochrome *c* were considered for analysis, as the electrostatic interactions between phosphate/succinate moieties in α-TOP/α-TOS and positively charged residues of cytochrome *c* play a major role in complex formation. The best ligand-bound receptor structure in each case was chosen based on lowest energy as well as the total number of conformations in that site. The interactions made by hydrophobic moieties in TOC analogues were ignored completely in this analysis as it is not clear whether they are presented as single ligands or as micelles to cytochrome *c*. If they are presented as micelles rather than a single ligand then the hydrophobic tails in α-TOP/α-TOS are buried inside the micelle.

*Peroxidase Activity Measurements*—Assessments of cytochrome *c* peroxidase activity were performed in 20 mM HEPES buffer (pH 7.4) with 100 μM DTPA using fluorescence of resorufin (oxidation product of Amplex Red) ($\lambda_{ex}$ 570 nm; $\lambda_{em}$ 585 nm). 1 μM cytochrome *c* was incubated with DOPC/TOCL liposomes for 10 min. Then 50 μM Amplex Red and 50 μM $H_2O_2$ were added, and the incubation proceeded for an additional 20 min (reaction rate was linear in the entire time interval). Fluorescence was detected by employing a Fusion α universal microplate analyzer and by using an excitation filter 535/25 nm and emission filter 590/20 nm.

Assessment of peroxidase activity of cytochrome *c* using fatty acid hydroperoxide as a source of oxidative equivalents for this reaction was performed by employing a Shimadzu RF5301-PC spectrofluorometer (Shimadzu, Japan). Cytochrome *c* was incubated with TOC analogues, or DOPC/TOCL liposomes for 10 min. Peroxidase reaction was started by addition of Amplex Red (50 μM) and $^{13}$S-HpODE (2.5 μM) For better characterization of the reaction rate in these conditions, which was very high, we chose to decrease the concentration of cytochrome *c* to 0.2 μM (*versus* 1 μM used in the reaction fueled by $H_2O_2$) and presented the initial reaction rate as the change in the fluorescence intensity during 10 s of incubation calculated during the first minute of incubation when the reaction was linear over time.

Peroxidase activity of mitochondria was assessed after their incubation with liposomes containing DOPE/sphingomyelin/α-TOS (9:2:1) or cholesterol/polyethylene glycol-phosphatidylethanolamine conjugated with the triphenylphosphonium group (DOPC/cholesterol/triphenylphosphonium/PEG/PE/α-TOS (6:2.5:0.6:1)) in 100 μl of MSH buffer without EDTA for 45 min at 37 °C. Incubation with triphenylphosphonium containing liposomes was performed in a buffer containing also 5 mM malate, 5 mM glutamate. Peroxidase activity of mitochondria (final concentration 0.25 mg of protein/ml) incubated with liposomes was determined in the presence of Amplex Red (50 μM) and tBOOH (2 mM) by measuring fluorescence of resorufin, an oxidation product of Amplex Red. Fluorescence was measured using a Shimadzu RF5301-PC spectrofluorometer (at excitation and emission wavelengths of 570 and 582 nm, respectively).

*Absorption Spectroscopy*—Optical spectra were recorded in 20 mM HEPES buffer (pH 7.4) using UV160U spectrophotometer (Shimadzu, Japan) and a 50-μl cuvette. For measurements of absorbance at 695 nm, the concentration of cytochrome *c* was 50 μM. The absorbance in the 650–750 nm area is strongly affected by a broad shoulder of the strong 550 nm peak. We approximated this by slowly changing the absorption shoulder with a linear function and subtracted the linear fit from the total spectrum. For quantitative assessment of the changes in the formation of high spin iron we used the height of peak at about 620 nm calculated by subtraction of absorbance reading at 675 nm from absorbance reading at 620 nm. Concentration of cytochrome *c* in these experiments was 75 μM. Due to significant interference of light scattering, the baseline was subtracted from each individual spectrum before obtaining the differential spectra.

*Cell Culture*—Mouse embryonic cytochrome $c^{-/-}$ cells (ATCC) and cytochrome $c^{+/+}$ cells (courtesy of Dr. Xiaodong Wang, Department of Biochemistry, University of Texas, Southwestern Medical Center, Dallas, TX) were cultured in DMEM supplemented with 15% FBS, 25 mM HEPES, 50 mg/liter of uridine, 110 mg/liter of pyruvate, 2 mM glutamine, 1× nonessential amino acids, 2′-mercaptoethanol, 0.5 × $10^6$ units/liter of mouse leukemia inhibitory factor, and 100 units/ml of penicillin and streptomycin. Cytochrome $c^{-/-}$ and cytochrome $c^{+/+}$

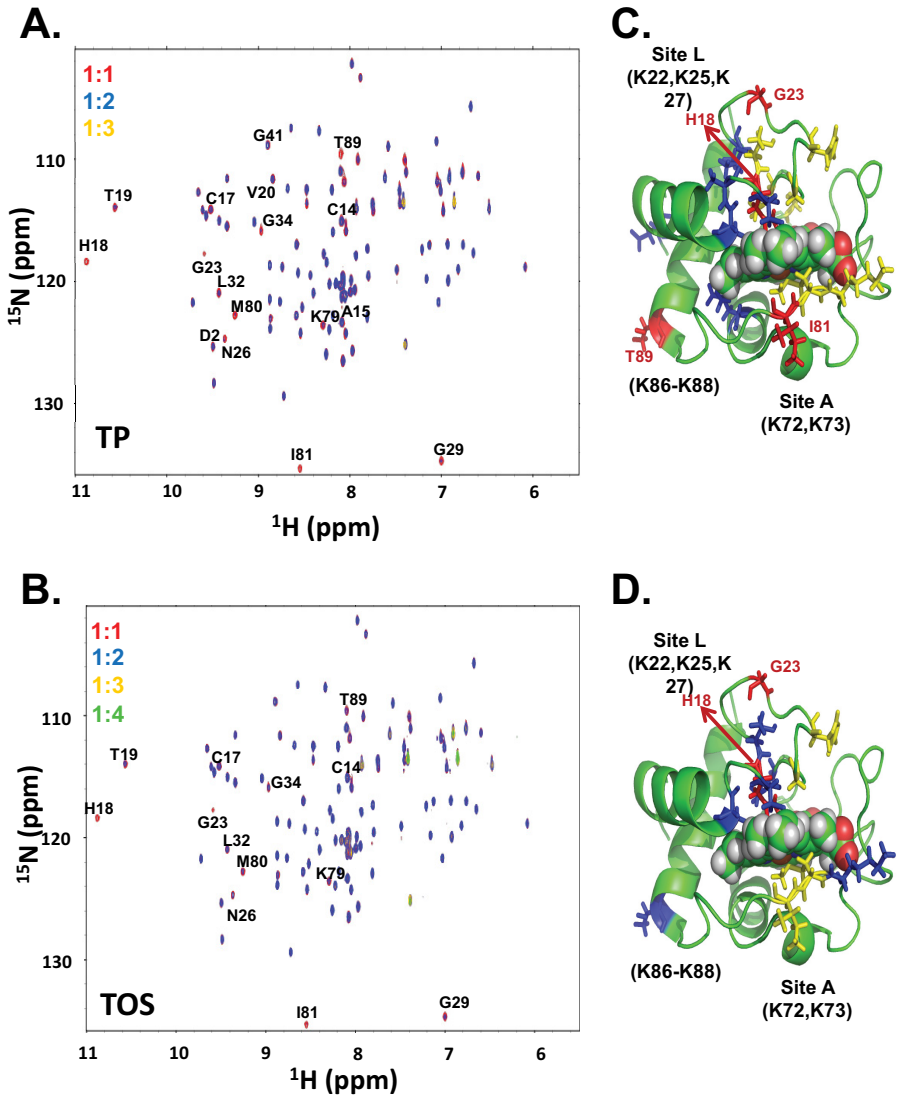


FIGURE 2. **NMR studies of cytochrome *c* and TOC analogues, α-TOP and α-TOS.** *A*, an overlay of $^{15}$N-$^{1}$H HSQC spectra of cytochrome *c* in HEPES buffer (pH 7.4) at 1:0 (*blue*), 1:2 (*red*), and 1:3 (*gold*) cytochrome *c* to α-TOP ratios. *B*, an overlay of $^{15}$N-$^{1}$H HSQC spectra of cytochrome *c* in HEPES buffer (pH 7.4) at 1:0 (*blue*), 1:2 (*red*), 1:3 (*green*), and 1:4 (*yellow*) cytochrome *c* to α-TOS ratios. Mapping of the signals that either disappeared (*red*) or exhibited significant (*yellow*) or moderate (*blue*) line broadening effects (*yellow*) at a ratio of 1:2 cytochrome *c* to α-TOP (*C*) and α-TOS (*D*) are mapped onto the structure of cytochrome *c*.

mouse embryonic cells were exposed to mito-VES alone or together with $H_2O_2$ (75 μM) for 16 h at 37 °C.

*Apoptosis Analysis*—At the end of incubation, cells were trypsinized and pooled with cells that had already been detached. The externalization of PS was determined by flow cytometry using an annexin V/FITC/propidium iodide kit (Biovision, Mountain View, CA). Cell debris represented by distinct low forward and side scatter were gated out for analysis. Ten thousand events were collected on a FACScanto II flow cytometer (BD Bioscience) equipped with Diva software. Percentages of annexin V-positive cells were calculated by combining annexin $V^+$/propidium $iodide^-$ (early apoptotic) and annexin $V^+$/propidium $iodide^+$ (late apoptotic or necrotic) cells.

*Statistical Analysis*—Data are expressed as mean ± S.D. of at least triplicate determinations. Changes in variables were analyzed by a one-way analysis of variance for multiple comparisons. Differences were considered significant at $p < 0.05$.

## RESULTS

*Interaction Sites of α-TOS/α-TOP on Cytochrome c*—To identify binding sites of tocopherol analogues on cytochrome *c*, we monitored interactions of α-TOP and α-TOS (Fig. 2) with the protein using NMR spectroscopy. Two-dimensional $^{1}$H-$^{15}$N HSQC spectra of cytochrome *c* acquired in the absence and presence of increasing amounts of α-TOP or α-TOS exhibited marked decreases in the intensity of numerous amide (NH) resonance signals. This is due to the enhanced line broadening effect of the NH signals in response to α-TOP/α-TOS binding to cytochrome *c*. An overlay of $^{1}$H-$^{15}$N HSQC spectra of cytochrome *c* at varying cytochrome *c*:α-TOS (1:1, 1:2, 1:3, and 1:4) and cytochrome *c*:α-TOP (1:1, 1:2, and 1:3) ratios is shown in Fig. 2. The NH resonance signals did not change at the 1:1 ratio of cytochrome *c*:α-TOP, whereas a 2-fold excess of α-TOP over cytochrome *c* made the signals corresponding to residues $His^{18}$, $G1y^{23}$, $Ile^{81}$, and $Thr^{89}$ disappear (Fig. 2*A*). Furthermore, the

signals corresponding to residues Thr[19], H26N, Gly[29], Leu[32], Gly[34], Lys[79], and Met[80] showed a significant decrease (>65%) in their intensities (Fig. 2*C*, residues colored in *yellow*). Compared with NH signals in the absence and presence of α-TOP at a 1:1 ratio to cytochrome *c*, a slight decrease in intensity was observed in signals corresponding to a set of 6 residues at the 1:2 ratio of cytochrome *c*:α-TOP (Fig. 2, *A* and *B*, residues colored in *red*). In addition to the signals that disappeared at a cytochrome *c*:α-TOP ratio of 1:2, the chemical shifts corresponding to almost all residues, with the exception of Glu[104], disappeared completely at a cytochrome *c*:α-TOP ratio of 1:3. Moreover, the NH signals corresponding to the side chains, around 7 ppm, also disappeared at a cytochrome *c*:α-TOP ratio of 1:3, suggesting binding of α-TOP to cytochrome *c*. Although a total of signals from four residues disappeared upon addition of a 2 times larger amount of α-TOP over cytochrome *c*, addition of 2 times excess α-TOS over cytochrome *c* only resulted in the complete disappearance of His[18] and Gly[23] NH resonance signals (Fig. 2*B*). Furthermore, a set of 11 residues showed a significant decrease (>55%) in their signal intensities (Fig. 2*D*, residues colored in *yellow* and *blue*). In addition, all NH signals, with the exception of chemical shifts corresponding to residues Glu[4], Lys[5], H33N, Lys[39], Ala[51], Tyr[67], and Glu[104], disappeared completely at a cytochrome *c*:α-TOS ratio of 1:3 (Fig. 2*B*, peaks in *yellow*). Titration with α-TOP and α-TOS beyond 2- and 3-fold excess over cytochrome *c*, respectively, resulted in complete disappearance of the amide backbone signals, with the exception of Glu[104] and for some side chain signals around 7 ppm. Although the overall chemical shift perturbation patterns observed in cytochrome *c* signals upon addition of α-TOP and α-TOS were similar, the interaction of cytochrome *c* with α-TOP was stronger than with α-TOS, as lower amounts of α-TOP were required for inducing the effects similar to those of α-TOS (Fig. 2, *A* and *B*).

The signals from the residues of cytochrome *c* that either disappeared or experienced enhanced line broadening upon titrating 2 times excess α-TOP/α-TOS are highlighted in the cytochrome *c* structure (Fig. 2, *C* and *D*). These residues are mostly localized to the proximal and distal ends of the heme. Some of the perturbed residues were also localized to regions that participate in hydrophobic interaction with the heme moiety, in line with previous studies where CL binding to cytochrome *c* was shown to significantly perturb the heme microenvironment (31).

*Absorbance at 695 nm*—To further characterize interactions of α-TOS and α-TOP with cytochrome *c* and unfolding of cytochrome *c* in the presence of these compounds, we employed measurements of absorbance at 695 nm. This characteristic absorption band is associated with an axial coordination of the heme iron in cytochrome *c* by the sulfur atom of Met[80] (Fe-S(Met[80])). The Fe-S(Met[80]) bond is not very strong (32) and is located in an unstable region of the protein (33, 24). Unfolding of cytochrome *c* is accompanied by rupture of this bond and decrease in absorbance at 695 nm. We found that incubation of cytochrome *c* with increasing amounts of α-TOS resulted in decreased 695 nm absorbance (Fig. 3). Relatively high concentrations of α-TOS (α-TOS:cytochrome *c* ratio, 15:1) were required to disrupt 50% of Fe-S(Met[80]) bonding. Notably,

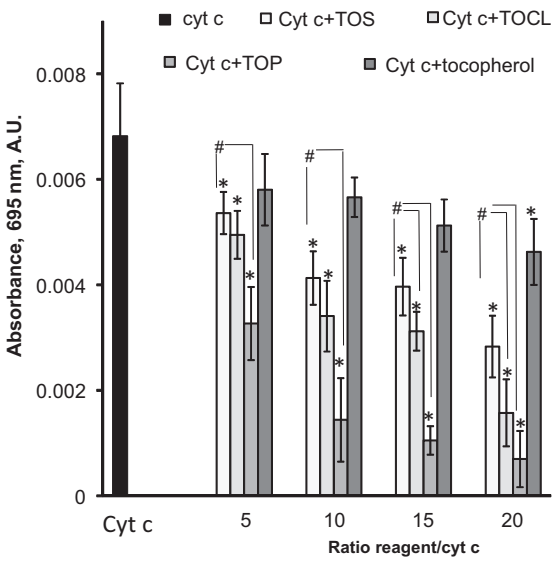


FIGURE 3. **Dependence of the absorbance of the Fe-S(Met[80]) bond (λ 695 nm) on the TOCL/TOC analogues ratio to cytochrome *c*.** The absorbance was measured in 20 mM HEPES buffer containing 100 μM DTPA (pH 7.4) using 50 μM of cytochrome *c* (*cyt c*), $n = 7–9$, *, $p < 0.05$ *versus* control; #, $p < 0.05$.

α-TOP exhibited a much stronger ability to disrupt the Fe-S(Met[80]) bond, eliminating 50% of the 695 nm absorbance at a α-TOP:protein ratio of 5:1. α-TOC, devoid of negatively charged moiety, had a significantly weaker effect than either of its derivatives, suppressing the absorbance by 30% at a ratio of 20:1.

*Assessment of High Spin Iron State*—Breaking of the iron-Met[80] sulfur bond causes the transition of hexa-coordinated heme iron configuration into penta-coordinated and leads to the appearance of high spin heme iron due to decreased *d*-orbital splitting. This is diagnostic of a molten globule organization of the hemo-protein that is characteristic of many non-native cytochrome *c* states induced by guanidine hydrochloride, low pH, and elevated temperature, or formed when cytochrome *c* binds to anionic phospholipid vesicles, micelles, polyanions, and electrodes. This high spin heme iron was also found in microperoxidases produced by tryptic digestion of cytochrome *c* resulting in the loss of the sixth coordination bond and markedly elevated peroxidase activity (34, 35). Therefore we used electronic absorption spectroscopy to spectrally distinguish between the high spin and low spin ferric hemes (36–39). We found that the presence of increasing amounts of α-TOS resulted in the formation of a new relatively weak band at about 620 nm, a slight intensity increase at about 495 nm, and a more pronounced shoulder at about 560 nm (Fig. 4*A*). The differential absorption spectra created by subtracting spectra of cytochrome *c* from spectra of cytochrome *c* incubated with α-TOS demonstrated positive peaks at 480–495 and 610–625 nm accompanied by a clear trough at ~700 nm (Fig. 4*B*, *inset*). These changes point to the formation of high spin iron, which parallel an intensity decrease of the 695 nm absorption band indicating breakage of the Fe-Met[80] bond. Quantitatively, both α-TOP and α-TOS induced concentration-dependent formation of high spin iron (Fig. 4*B*), whereby the effects of the former were greater than those of the latter. TOCL was more effective

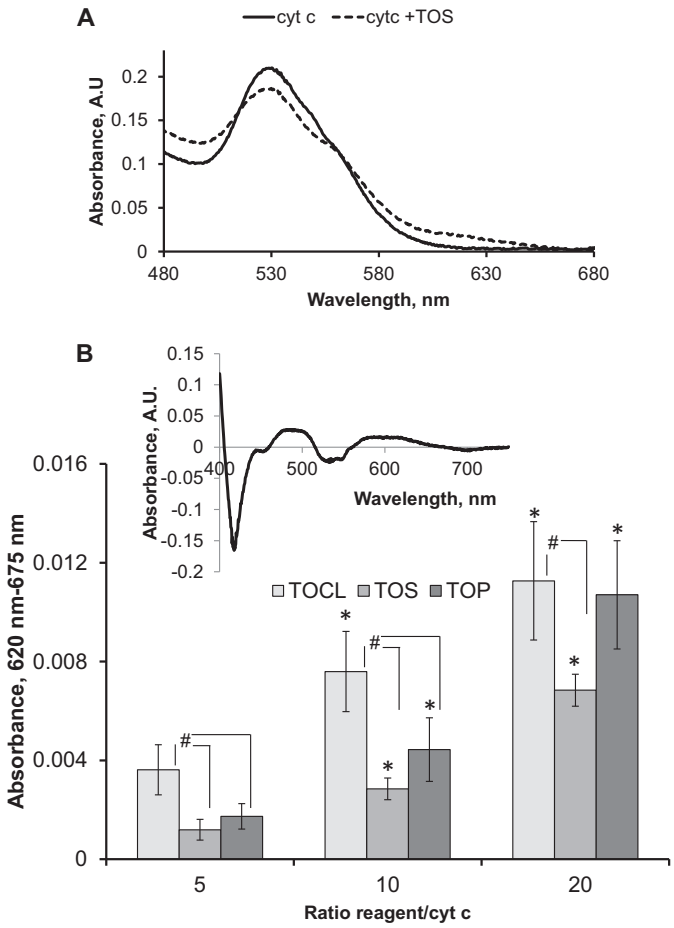


FIGURE 4. **Effect of TOCL, α-TOS, and α-TOP on the formation of heme iron high spin form.** *A*, UV-visible absorption spectra of ferric cytochrome *c* in the presence and absence of α-TOS in a α-TOS/cytochrome *c* ratio of 20:1. *B*, effect of TOCL, α-TOS, and α-TOP on the height of peak at about 620 nm. *Inset*, the differential absorption spectrum created by subtracting spectrum of cytochrome *c* from the spectrum of cytochrome *c* incubated with α-TOS showing positive features at ~490 and ~600 nm indicative of high spin ferric heme. Spectra were recorded in 20 mM HEPES buffer containing 100 μM DTPA (pH 7.4) using 75 μM of cytochrome *c*, $n = 4–7$; *, $p < 0.05$ *versus* samples containing the same reagent in ratio reagent/cytochrome *c*, 5:1; #, $p < 0.05$

than α-TOP and α-TOS as an inducer of the high spin iron especially at lower ratios to cytochrome *c*.

*Molecular Docking Studies*—To more accurately characterize α-TOS and α-TOP interaction sites on cytochrome *c*, we performed molecular docking studies using the three-dimensional structure of native horse heart cytochrome *c* (PDB code 1OCD). The predicted conformations that have at least one positively charged residue on cytochrome *c* in close proximity to negatively charged groups of α-TOP or α-TOS are shown in Fig. 5. The binding of α-TOP and α-TOS to cytochrome *c* exhibited key differences in both predicted binding energies as well as their interaction sites on cytochrome *c*. The predicted binding energies for α-TOP and α-TOS were −4.3 and −5.6 Kcal/mol, respectively. In the case of α-TOP, the phosphate group was predicted to bind in close proximity (<5 Å) to residues $Lys^{72}$ and $Lys^{73}$. Strikingly, α-TOS was predicted to localize to a different site on cytochrome *c*. The negatively charged succinate moiety of α-TOS preferentially binds in close proximity to $Lys^{22}$ and $Lys^{25}$. These two binding sites are similar to previously proposed putative CL binding sites on cytochrome *c*

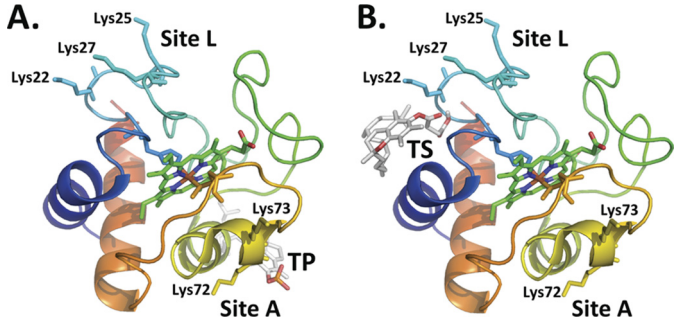


FIGURE 5. **Predicted binding sites of TOC analogues on cytochrome *c*.** The predicted binding poses of (*A*) phosphate moiety of α-TOP in close proximity to $Lys^{72}$ and $Lys^{73}$, and (*B*) succinate group of α-TOS in close proximity to $Lys^{22}$, $Lys^{25}$, and $Lys^{27}$. The residues corresponding to the two putative CL binding sites, site A and site L are labeled and residues corresponding to these sites are rendered as *sticks*. The structure of cytochrome *c* is shown as a schematic and colored *red* to *blue* to indicate the N-C terminus. The ligand, heme of cytochrome *c* along with the two coordinating residues $His^{18}$ and $Met^{80}$ are rendered as *sticks*.

(20). The binding of negatively charged CL at site A was shown to be stabilized by positively charged residues $Lys^{72}$/$Lys^{73}$ (40, 41) and at site L by residues $Lys^{22}$/$Lys^{25}$/$Lys^{27}$ (42). The similarity in binding between CL and TOC analogues (α-TOP and α-TOS) further supports the ability of α-TOP/α-TOS to induce unfolding of cytochrome *c*, triggering its peroxidase activity.

*Peroxidase Activity*—If interactions of cytochrome *c* with negatively charged TOC derivatives induce protein unfolding accompanied by a loss of an axial ligand of heme iron, the resulting increased accessibility of the iron atom to small molecules like $H_2O_2$ should activate the "dormant" peroxidase function of the hemoprotein similar to the effects of CL and other anionic phospholipids (20). To experimentally assess the ability of α-TOS and α-TOP to stimulate peroxidase activity of cytochrome *c*, we performed measurements of oxidation of a prototypical phenolic substrate, Amplex Red, to its product, resorufin. Both α-TOS and α-TOP were able to activate cytochrome *c* as a peroxidase as evidenced by the enhanced accumulation of resorufin. α-TOS exhibited a higher activating potential than α-TOP and, at higher concentrations, α-TOS was comparable with TOCL (Fig. 6*A*). Interestingly, in the presence of TOCL, the stimulatory effect of TOS was not apparent (Fig. 6*B*). As an alternative to the $H_2O_2$ source of oxidizing equivalents, we tested the fatty acid hydroperoxide, $^{13}$S-hydroperoxy-9*Z*,11*E*-octadecadienoic acid (FFA-OOH). FFA-OOH and $H_2O_2$ have different binding sites on the cytochrome *c* molecule: $H_2O_2$ was found to occupy a site in the proximity to $His^{18}$, whereas FFA-OOH binds to a different site, with the hydroperoxy group located in proximity to $Arg^{38}$ and $His^{33}$ (43). In line with previously reported data, FFA-OOHs were much better peroxidase substrates for cytochrome *c*/TOCL than $H_2O_2$, whereas the peroxidase activity of cytochrome *c* was only slightly increased by α-TOS and remained essentially unaffected by α-TOP (Fig. 7).

We further assessed the effect of α-TOS on the peroxidase activity of rat liver mitochondria induced by tert-butyl hydroperoxide (tBOOH). To improve delivery of α-TOS into the mitochondrial interior, the reagent was incorporated into liposomes containing DOPE, which is a fusogenic lipid commonly used in drug delivery, and sphingomyelin. Results of

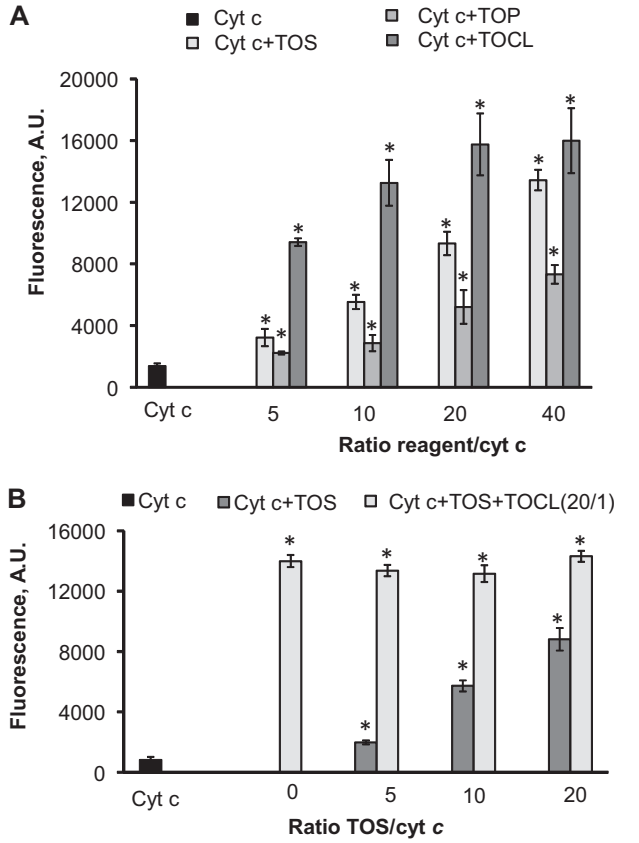


FIGURE 6. **Peroxidase activity of cytochrome *c* triggered by α-TOS and α-TOP assessed by $H_2O_2$-induced oxidation of Amplex Red.** *A*, comparison of TOCL, α-TOS, and α-TOP as activators of peroxidase function of cytochrome *c*. *B*, effect of simultaneous addition of α-TOS and TOCL on peroxidase activity of cytochrome *c*. *Dark gray columns* correspond to the samples containing TOS only, *light gray columns* represent the samples containing different amounts of TOS plus TOCL (constant amount) thus yielding the same ratio of TOCL/cytochrome *c*, 20:1, but varying ratios of TOS/cytochrome *c* (*cyt c*). Measurements were performed in 20 mM HEPES buffer (pH 7.4) with 100 μM DTPA; the concentration of cytochrome *c* was 1 μM, concentrations of Amplex Red and $H_2O_2$ were 50 μM. Samples containing cytochrome *c*, Amplex Red, and $H_2O_2$ were used as a control. $n = 6$ experiments; *, $p < 0.05$ *versus* cytochrome *c*.

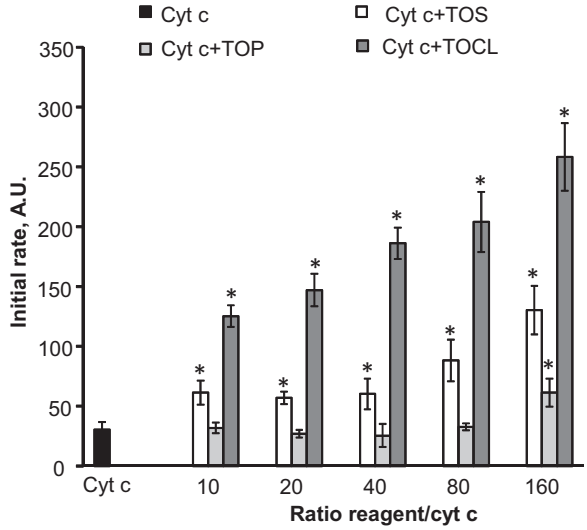


FIGURE 7. **Effect of TOCL, α-TOS, and α-TOP on peroxidase activity of cytochrome *c* in the presence of $^{13}$S-HpODE.** Measurements were performed in 20 mM HEPES buffer (pH 7.4) with 100 μM DTPA using 0.2 μM cytochrome *c*, 50 μM Amplex Red, and 2.5 μM $^{13}$S-HpODE, $n = 3$ experiments; *, $p < 0.05$ *versus* cytochrome *c* (*cyt c*). The control is the initial rate of peroxidase reaction catalyzed by cytochrome *c* in the presence of $^{13}$S-HpODE and Amplex Red.

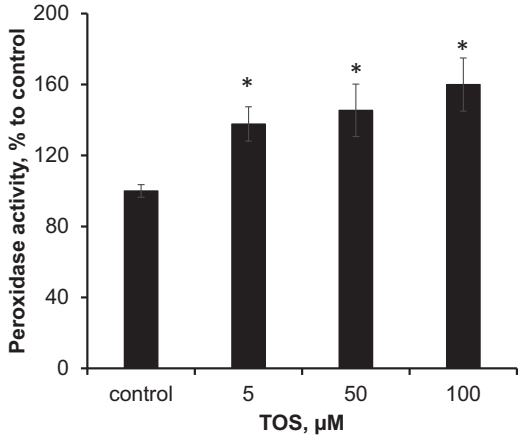


FIGURE 8. **Effect of α-TOS on peroxidase activity of rat liver mitochondria.** Mitochondria (0.9 mg of protein/ml) were incubated with liposomes containing DOPE/sphingomyelin/α-TOS (9:2:1) in 100 μl of MIB buffer without EGTA for 45 min at 37 °C. Peroxidase activity was determined in the presence of Amplex Red (50 μM) and tBOOH (2 mM), by measuring the fluorescence of resorufin, an oxidation product of Amplex Red. The final concentration of P2 fraction was 0.25 mg of protein/ml. Data are mean ± S.D., $n = 3$; *, $p < 0.05$ *versus* control.

these experiments demonstrated that α-TOS activated peroxidase activity of mitochondria in a concentration-dependent manner (Fig. 8). Similar results were obtained using an alternative protocol for improved delivery of α-TOS into mitochondria: its incorporation into liposomes containing triphenylphosphonium/PEG/PE, known to readily accumulate in mitochondria (44). In this case, α-TOS caused a 150% increase of peroxidase activity.

*Apoptosis Analysis*—Assuming that peroxidase activation of cytochrome *c* is required for the execution of apoptotic program (20), we studied the effects of α-TOS on apoptosis in mouse embryonic wild type (cytochrome $c^{+/+}$) cells and cytochrome $c^{-/-}$ cells. To target α-TOS into mitochondria, we employed its triphenylphosphonium conjugate, mito-VES, and assessed PS externalization as a hallmark of apoptosis (45). $H_2O_2$ (75 μM) was utilized as an inducer of apoptosis and a source of oxidizing equivalents for the peroxidase activity of cytochrome *c*. We found that mito-VES, but not α-TOS, increased PS externalization in both cytochrome $c^{+/+}$ and cytochrome $c^{-/-}$ cells in a concentration-dependent manner. Notably, simultaneous addition of α-TOS and $H_2O_2$ resulted in a markedly stronger apoptosis in cytochrome $c^{+/+}$ cells than in cytochrome $c^{-/-}$ cells, whereas addition of $H_2O_2$ itself was insufficient for the apoptosis induction (Fig. 9). This indicates that the apoptogenic potential of mito-VES is dependent on the presence of cytochrome *c*, likely due to its peroxidase activity. These results are in line with the previously demonstrated markedly enhanced pro-apoptotic efficacy of mito-VES *versus* α-TOS (17).

## DISCUSSION

Vital role of cytochrome *c* in safeguarding the uninterrupted flow of electrons between respiratory complexes III and IV of

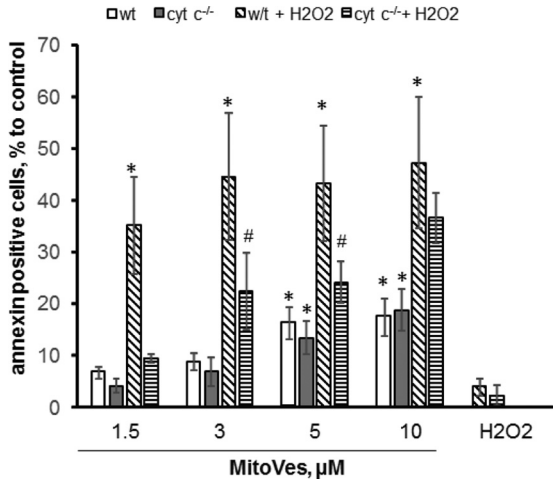


FIGURE 9. **Effect of mito-VES on apoptosis in mouse embryonic cytochrome $c^{-/-}$ and cytochrome $c^{+/+}$ cells.** Four samples were exposed to each of the mito-VES concentrations: two in the absence of $H_2O_2$ (the *first two bars*: empty, WT cells; *filled dark gray*, cytochrome $c^{-/-}$ (*cyt c*) cells, respectively) and two in the presence of $H_2O_2$ (75 $\mu$M) (*diagonally striped bars*, WT cells with $H_2O_2$; *horizontal striped bars*, cytochrome $c^{-/-}$ cells with $H_2O_2$) and incubated for 16 h at 37 °C. The cells were then collected and PS externalization was determined by flow cytometry using the annexin V-FITC/propidium iodide kit. Data are mean ± S.D., $n = 3$ experiments. *, $p < 0.05$ *versus* control cells; #, $p < 0.05$ *versus* cytochrome $c^{-/-}$ cells.

the mitochondrial respiratory chain has been challenged by the discoveries of its unexpected participation in cell death apoptotic pathways. This includes the involvement of cytochrome *c* as a peroxidase catalyst of CL peroxidation, required for the release of pro-apoptotic factors from mitochondria into the cytosol (18, 20), and as one of the factors facilitating the formation of apoptosomes and caspase activation (46). The dormant peroxidase function is conferred on cytochrome *c* by its interaction with a mitochondria-specific anionic phospholipid CL, normally asymmetrically confined to the inner mitochondrial membrane but redistributed to the outer membrane during apoptosis (with the likely participation of two candidate mitochondrial translocators: phospholipid scramblase-3 and nucleoside diphosphate kinase D (47, 48). Binding of CL to cytochrome *c* causes unfolding of the protein, thus paving the way for peroxy donors, $H_2O_2$ or organic (lipid) hydroperoxides, to the heme catalytic site (21). The resultant peroxidase activity displays significant specificity toward CLs, yielding its highly diversified oxygenated species and their hydrolysis products, predominantly mono-lyso-CLs and oxygenated fatty acids, with signaling modalities (49–51). CL hydroperoxides can be utilized by the peroxidase complex as an alternative (to $H_2O_2$) source of oxidizing equivalents, thus "perpetuating" the functioning of the peroxidase cycle (43, 47). Although the significance of the peroxidase activation of cytochrome *c* in apoptosis has been documented (18, 20), the uniqueness of CLs as endogenous activators is not unequivocal. Indeed, the structural requirements for the cytochrome *c* unfolding are relatively "loose," and it is possible that other molecules combining a hydrophobic chain with a negatively charged functionality may fulfill the requisite conditions (52–56). Therefore, we hypothesized that TOC analogues α-TOS and α-TOP may act as activators of cytochrome *c* peroxidase function.

A redox-silent compound α-TOS has been recently documented as an anti-cancer drug inducing apoptosis in several types of tumor (but not normal) cells (11, 16, 17). Mitochondria were shown to play a central role in α-TOS-induced apoptosis, and mitochondrial targeting of α-TOS by it tagging with the triphenylphosphonium group enhanced its pro-apoptotic effect (17). It was suggested that possible mechanisms of induction of apoptosis induced by α-TOS involves induction of reactive oxygen species production by its interaction with the ubiquinone-binding site of mitochondrial complex II (16, 17, 57). In addition, α-TOS demonstrated BH3 mimetic activity by blocking the interaction of the anti-apoptotic Bcl-2 family proteins with their pro-apoptotic counterparts (58). Our data are compatible with yet another possible mechanism of α-TOS involvement in the induction of apoptosis via its ability to unfold cytochrome *c* and induce its peroxidase activity. Indeed, we demonstrated that α-TOS, effectively delivered into mitochondria, activates their tBuOOH-dependent peroxidase activity.

Notably, mito-VES (added along with $H_2O_2$) displayed a markedly higher pro-apoptotic potential in mouse embryonic cytochrome $c^{+/+}$ cells compared with cytochrome $c^{-/-}$ cells, thus clearly demonstrating the dependence of its pro-apoptotic action on cytochrome *c*. It is possible that TOS-induced peroxidase activity of cytochrome *c* causes oxidation of CL. We found that binding of the negatively charged succinate moiety of α-TOS with cytochrome *c* occurs in close proximity to $Lys^{22}$ and $Lys^{25}$ (L-binding site) (42) leaving another site (site A) with $Lys^{72}$/$Lys^{73}$ (40, 41) still available for the interaction with CL. Thus an "alternatively" bound polyunsaturated CL can be a target for peroxidation by cytochrome *c*·α-TOS complex provided the source of oxidizing equivalents is available. However, binding of CL to cytochrome *c* is not always required for its oxidation. For example, 1 electron oxidation intermediates generated by the peroxidase activity of cytochrome *c*/α-TOS from a variety of phenolic compounds, phenoxyl radicals, can escape from the catalytic site and diffuse to the locales enriched with oxidizable lipid substrates, including those with the CL molecules. Thus, in the presence of phenolic compounds, however, the specificity of oxidation toward CL may not be high and other vulnerable substrates and reductants (*e.g.* other polyunsaturated lipids, thiols) can get oxidized (59). This phenomenon, the so-called extension of the peroxidase catalytic site, has been documented for several peroxidases with a variety of phenolic compounds with appropriate redox potentials (60) but it has not yet been described for cytochrome *c*.

α-TOP, in contrast to α-TOS, is ubiquitously present, albeit at rather low concentrations, in animal tissues as well as plants, and has been shown to be synthesized by cells (61, 62). Our results demonstrated that TOP, at a TOP:cytochrome *c* ratio of 20:1, increases peroxidase activity of cytochrome *c* by more than 3-fold. Given the importance of cytochrome *c* activation in the execution of apoptotic program (18), this suggests that TOP is a potential inducer of cytochrome *c*-dependent apoptosis. In fact, the ability of TOP to induce apoptosis has been demonstrated in THP-1 monocytes and murine MG-63 melanoma cells (61, 63). However, this effect was observed only at TOP concentrations >50 $\mu$M. Although the requirement of high

concentrations of exogenously added TOP for its pro-apoptotic effect can be explained by the fact that only a small fraction of it partitions into the mitochondrial intermembrane space to form a peroxidase complex with cytochrome *c*, the question still remains whether intracellular TOP concentrations are sufficient for triggering apoptosis. In tissues of unsupplemented animals and humans, the basal α-TOP level was estimated as ~0.2 μM (64). After supplementation with α-TP at a dose of 1.33 g/kg body weight for 4 weeks, this level was increased more than 100-fold to 29.4 μM. Thus, endogenous levels of TOP are too low to expect its significant contribution to apoptotic cell death. However, its pharmacological effects may be due, at least in part, to its ability, at higher concentrations, to facilitate cell death pathways.

Our structural studies, including heteronuclear NMR assessments, of intactness of $Met^{80}$-Fe coordination bond, and high spin iron, along with the computer simulations, demonstrated that α-TOS and α-TOP, similarly to TOCL, interacted with cytochrome *c* and induced its unfolding. Thus both α-TOS and α-TOP can act as peroxidase activators, whereas the non-esterified parental compound, TOC, devoid of a negatively charged functionality, did not demonstrate this ability. However, there were substantial differences in the binding sites and the abilities of α-TOS and α-TOP to induce structural re-arrangements in cytochrome *c*. Molecular docking calculations demonstrated that the negatively charged succinate moiety of α-TOS was preferentially bound in close proximity to $Lys^{22}$ and $Lys^{25}$ (site L), whereas a more hydrophilic α-TOP was predicted to localize to a different site on cytochrome *c* electrostatically interacting with $Lys^{72}$ and $Lys^{73}$ (site A). $Lys^{72}$ and $Lys^{73}$ are, in particular, implicated as candidate replacement ligands of $Met^{80}$ during alkaline transition of cytochrome *c* and are thought to participate in electrostatic binding to anionic phospholipids. The predicted binding energy of α-TOP was lower than that of α-TOS. NMR studies indicated that α-TOP was a stronger modifier of cytochrome *c* structure than α-TOS. Similarly, α-TOP was more effective in disrupting the $Met^{80}$-Fe bond and inducing accumulation of the high spin form of the hemoprotein.

Peroxidase activity measurements demonstrated the effectiveness of α-TOS and TOCL in activation of peroxidase activity of cytochrome *c*. Notably, computationally predicted similarity in cytochrome *c* binding sites for α-TOS and TOCL, and the lack of additive effects on peroxidase activity suggest that similar "unfolding" mechanisms may be triggered by these compounds. At the same time, mechanisms of activation of cytochrome *c* peroxidase activity by TOCL and α-TOS are not entirely identical as illustrated by differential responses of the respective cytochrome *c* complexes with either TOCL or α-TOS to FFA-OOH as a substrate for the peroxidase reaction. Interestingly, α-TOP demonstrated a much weaker potency as a peroxidase activator of cytochrome *c* than either α-TOS or TOCL. Apparent discrepancy between the markedly decreased absorbance at 695 nm along with its ability to trigger stronger changes in NH signals, characterizing rupture of the Fe-S($Met^{80}$) bond, and small activation of peroxidase activity by α-TOP can be explained by different mechanisms involved. Although peroxidase activation requires a perturbation of the cytochrome *c* structure that allows access and interaction of small $H_2O_2$ molecules with the heme iron catalytic site, complete rupture of the Fe-S($Met^{80}$) bond is not obligatory. Moreover, differences in effects of α-TOP and α-TOS on unfolding of cytochrome *c* and its peroxidase activity can be explained by specificities of their binding with cytochrome *c* to $Lys^{72}$/$Lys^{73}$ (site A) and $Lys^{22}$/$Lys^{25}$ (site L), respectively.

In α-TOS molecule, the hydroxy group in position 6 of its chromanol ring, required for the radical scavenging activity, is esterified with succinate. Because α-TOS activation of cytochrome *c* into a peroxidase is mainly due to a partial protein unfolding (Figs. 2 and 3), rather than chemical interactions with the protein, it is unlikely that significant oxidation of α-TOS takes place. Notably, α-TOS itself has no antioxidant properties and does not undergo oxidation (65). However, the esterified succinic acid moiety can be removed by cellular esterases thereby generating α-tocopherol. It was suggested that a comparatively higher esterase activity of normal cells *versus* low or negligible activity found in cancer cells can be responsible for the higher selectivity of α-TOS toward malignant cells (66, 67). Thus formed tocopherol is prone to oxidative modifications but, in the absence of the succinic moiety, is incapable of inducing the peroxidase activity. Thus, it seems unlikely that cytochrome *c* can oxidize α-TOS.

In summary, using computational modeling and NMR studies, we demonstrate that α-TOS and α-TOP interact with cytochrome *c* at similar sites previously proposed for CL. Absorption spectroscopy showed that both α-TOS and α-TOP effectively disrupt the Fe-S($Met^{80}$) bond indicating the unfolding of cytochrome *c*. By measuring the oxidation of a typical peroxidase substrate, Amplex Red, we showed that α-TOS and α-TOP can stimulate peroxidase activity of cytochrome *c*. Overall, the structural analysis indicates that "peroxidase" activation of cytochrome *c* may be achieved via several different unfolding pathways with specific enzymatic features. It is also possible that these distinctive peroxidase "subspecies" of cytochrome *c* would entertain different catalytic mechanisms, *e.g.* with alternate proportions of hemolytic *versus* heterolytic activation of peroxide substrates, resulting in diversified stereospecificity of CL peroxidation products. Physiologically, the significance of these alternate pathways may be realized through the hydrolysis of peroxidized CL leading to the production of different lipid mediators, oxygenated fatty acids, and oxygenated or non-oxygenated lyso-CLs with yet to be explored signaling functions (51). α-TOS (and its mitochondrially targeted counterpart, mito-VES) and α-TOP can serve as activators of peroxidase activity of cytochrome *c* leading to CL oxidation as a step in the execution of the apoptotic program. These data may be instrumental in targeted design of novel regulators/activators of peroxidase activity of cytochrome *c* with desirable functions.

## REFERENCES

1. Evans, H. M., and Bishop, K. S. (1922) On the existence of a hitherto unrecognized dietary factor essential for reproduction. *Science* **56,** 650–651
2. Tappel, A. L. (1970) Biological antioxidant protection against lipid peroxidation damage. *Am. J. Clin. Nutr.* **23,** 1137–1139
3. Packer, L. (1991) Protective role of vitamin E in biological systems. *Am. J. Clin. Nutr.* **53,** 1050S–1055S

4. Niki, E., and Traber, M. G. (2012) A history of vitamin E. *Ann. Nutr. Metab.* **61,** 207–212
5. Myung, S. K., Ju, W., Cho, B., Oh, S. W., Park, S. M., Koo, B. K., Park, B. J., and Korean Meta-Analysis Study, G. (2013) Efficacy of vitamin and antioxidant supplements in prevention of cardiovascular disease: systematic review and meta-analysis of randomised controlled trials. *BMJ* **346,** f10
6. Dolara, P., Bigagli, E., and Collins, A. (2012) Antioxidant vitamins and mineral supplementation, life span expansion and cancer incidence: a critical commentary. *Eur. J. Nutr.* **51,** 769–781
7. Abner, E. L., Schmitt, F. A., Mendiondo, M. S., Marcum, J. L., and Kryscio, R. J. (2011) Vitamin E and all-cause mortality: a meta-analysis. *Curr Aging Sci* **4,** 158–170
8. Ricciarelli, R., Zingg, J. M., and Azzi, A. (2001) Vitamin E: protective role of a Janus molecule. *FASEB J.* **15,** 2314–2325
9. Kagan, V. E. (1989) Tocopherol stabilizes membrane against phospholipase A, free fatty acids, and lysophospholipids. *Ann. N.Y. Acad. Sci.* **570,** 121–135
10. Galli, F., and Azzi, A. (2010) Present trends in vitamin E research. *BioFactors* **36,** 33–42
11. Neuzil, J., Weber, T., Gellert, N., and Weber, C. (2001) Selective cancer cell killing by α-tocopheryl succinate. *Br. J. Cancer* **84,** 87–89
12. Rohlena, J., Dong, L. F., Ralph, S. J., and Neuzil, J. (2011) Anticancer drugs targeting the mitochondrial electron transport chain. *Antioxid. Redox Signal.* **15,** 2951–2974
13. Negis, Y., Zingg, J. M., Libinaki, R., Meydani, M., and Azzi, A. (2009) Vitamin E and cancer. *Nutr. Cancer* **61,** 875–878
14. Azzi, A. (2007) Molecular mechanism of α-tocopherol action. *Free Radic. Biol. Med.* **43,** 16–21
15. Kogure, K., Manabe, S., Hama, S., Tokumura, A., and Fukuzawa, K. (2003) Potentiation of anti-cancer effect by intravenous administration of vesiculated α-tocopheryl hemisuccinate on mouse melanoma *in vivo*. *Cancer Lett.* **192,** 19–24
16. Ralph, S. J., Moreno-Sánchez, R., Neuzil, J., and Rodríguez-Enríquez, S. (2011) Inhibitors of succinate: quinone reductase/complex II regulate production of mitochondrial reactive oxygen species and protect normal cells from ischemic damage but induce specific cancer cell death. *Pharm. Res.* **28,** 2695–2730
17. Dong, L. F., Jameson, V. J., Tilly, D., Cerny, J., Mahdavian, E., Marín-Hernández, A., Hernández-Esquivel, L., Rodríguez-Enríquez, S., Stursa, J., Witting, P. K., Stantic, B., Rohlena, J., Truksa, J., Kluckova, K., Dyason, J. C., Ledvina, M., Salvatore, B. A., Moreno-Sánchez, R., Coster, M. J., Ralph, S. J., Smith, R. A., and Neuzil, J. (2011) Mitochondrial targeting of vitamin E succinate enhances its pro-apoptotic and anti-cancer activity via mitochondrial complex II. *J. Biol. Chem.* **286,** 3717–3728
18. Kagan, V. E., Tyurin, V. A., Jiang, J., Tyurina, Y. Y., Ritov, V. B., Amoscato, A. A., Osipov, A. N., Belikova, N. A., Kapralov, A. A., Kini, V., Vlasova, I. I., Zhao, Q., Zou, M., Di, P., Svistunenko, D. A., Kurnikov, I. V., and Borisenko, G. G. (2005) Cytochrome *c* acts as a cardiolipin oxygenase required for release of proapoptotic factors. *Nat. Chem. Biol.* **1,** 223–232
19. Paradies, G., Petrosillo, G., Paradies, V., and Ruggiero, F. M. (2009) Role of cardiolipin peroxidation and $Ca^{2+}$ in mitochondrial dysfunction and disease. *Cell Calcium* **45,** 643–650
20. Kagan, V. E., Bayir, H. A., Belikova, N. A., Kapralov, O., Tyurina, Y. Y., Tyurin, V. A., Jiang, J., Stoyanovsky, D. A., Wipf, P., Kochanek, P. M., Greenberger, J. S., Pitt, B., Shvedova, A. A., and Borisenko, G. (2009) Cytochrome *c*/cardiolipin relations in mitochondria: a kiss of death. *Free Radic. Biol. Med.* **46,** 1439–1453
21. Kapralov, A. A., Kurnikov, I. V., Vlasova, I. I., Belikova, N. A., Tyurin, V. A., Basova, L. V., Zhao, Q., Tyurina, Y. Y., Jiang, J., Bayir, H., Vladimirov, Y. A., and Kagan, V. E. (2007) The hierarchy of structural transitions induced in cytochrome *c* by anionic phospholipids determines its peroxidase activation and selective peroxidation during apoptosis in cells. *Biochemistry* **46,** 14232–14244
22. Rumbley, J. N., Hoang, L., and Englander, S. W. (2002) Recombinant equine cytochrome *c* in *Escherichia coli*: high-level expression, characterization, and folding and assembly mutants. *Biochemistry* **41,** 13894–13901
23. Liu, W., Rumbley, J., Englander, S. W., and Wand, A. J. (2003) Backbone and side-chain heteronuclear resonance assignments and hyperfine NMR shifts in horse cytochrome *c*. *Protein Sci.* **12,** 2104–2108
24. Krishna, M. M., Maity, H., Rumbley, J. N., Lin, Y., and Englander, S. W. (2006) Order of steps in the cytochrome *c* folding pathway: evidence for a sequential stabilization mechanism. *J. Mol. Biol.* **359,** 1410–1419
25. Maity, H., Rumbley, J. N., and Englander, S. W. (2006) Functional role of a protein foldon: an ω-loop foldon controls the alkaline transition in ferricytochrome *c*. *Proteins* **63,** 349–355
26. Krishna, M. M., Maity, H., Rumbley, J. N., and Englander, S. W. (2007) Branching in the sequential folding pathway of cytochrome *c*. *Protein Sci.* **16,** 1946–1956
27. Pallotti, F., and Lenaz, G. (2007) Isolation and subfractionation of mitochondria from animal cells and tissue culture lines. *Methods Cell Biol.* **80,** 3–44
28. Johnson, B. A. (2004) Using NMRView to visualize and analyze the NMR spectra of macromolecules. *Methods Mol. Biol.* **278,** 313–352
29. Goddard, T., and Kneller, D. (2008) *SPARKY 3*, University of California, San Francisco, CA
30. Trott, O., and Olson, A. J. (2010) AutoDock Vina: improving the speed and accuracy of docking with a new scoring function, efficient optimization, and multithreading. *J. Comp. Chem.* **31,** 455–461
31. Sinibaldi, F., Fiorucci, L., Patriarca, A., Lauceri, R., Ferri, T., Coletta, M., and Santucci, R. (2008) Insights into cytochrome *c*-cardiolipin interaction. Role played by ionic strength. *Biochemistry* **47,** 6928–6935
32. Droghetti, E., Oellerich, S., Hildebrandt, P., and Smulevich, G. (2006) Heme coordination states of unfolded ferrous cytochrome *c*. *Biophys. J.* **91,** 3022–3031
33. Maity, H., Maity, M., Krishna, M. M., Mayne, L., and Englander, S. W. (2005) Protein folding: the stepwise assembly of foldon units. *Proc. Natl. Acad. Sci. U.S.A.* **102,** 4741–4746
34. Battistuzzi, G., Bortolotti, C. A., Bellei, M., Di Rocco, G., Salewski, J., Hildebrandt, P., and Sola, M. (2012) Role of Met80 and Tyr67 in the low-pH conformational equilibria of cytochrome *c*. *Biochemistry* **51,** 5967–5978
35. Oellerich, S., Wackerbarth, H., and Hildebrandt, P. (2002) Spectroscopic characterization of nonnative conformational states of cytochrome *c*. *J. Phys. Chem. B* **106,** 6566–6580
36. Marques, H. M. (2007) Insights into porphyrin chemistry provided by the microperoxidases, the haempeptides derived from cytochrome c. *Dalton Trans.* **39,** 4371–4385
37. Munro, O. Q., and Marques, H. M. (1996) Heme-peptide models for hemoproteins: 1. solution chemistry of *N*-acetylmicroperoxidase-8. *Inorg. Chem.* **35,** 3752–3767
38. Antonini, E., and Brunori, M. (1971) The derivatives of ferric hemoglobin and myoglobin. in *Hemoglobin and Myoglobin in Their Reactions with Ligands,* pp. 40–54, North Holland, Amsterdam
39. Carraway, A. D., McCollum, M. G., and Peterson, J. (1996) Characterization of *N*-acetylated heme undecapeptide and some of its derivatives in aqueous media: monomeric model systems for hemoproteins. *Inorg. Chem.* **35,** 6885–6891
40. Rytömaa, M., and Kinnunen, P. K. (1994) Evidence for two distinct acidic phospholipid-binding sites in cytochrome *c*. *J. Biol. Chem.* **269,** 1770–1774
41. Rytömaa, M., and Kinnunen, P. K. (1995) Reversibility of the binding of cytochrome *c* to liposomes: implications for lipid-protein interactions. *J. Biol. Chem.* **270,** 3197–3202
42. Kawai, C., Prado, F. M., Nunes, G. L., Di Mascio, P., Carmona-Ribeiro, A. M., and Nantes, I. L. (2005) pH-dependent interaction of cytochrome *c* with mitochondrial mimetic membranes: the role of an array of positively charged amino acids. *J. Biol. Chem.* **280,** 34709–34717
43. Belikova, N. A., Tyurina, Y. Y., Borisenko, G., Tyurin, V., Samhan Arias, A. K., Yanamala, N., Furtmüller, P. G., Klein-Seetharaman, J., Obinger, C., and Kagan, V. E. (2009) Heterolytic reduction of fatty acid hydroperoxides by cytochrome *c*/cardiolipin complexes: antioxidant function in mitochondria. *J. Am. Chem. Soc.* **131,** 11288–11289
44. Biswas, S., Dodwadkar, N. S., Deshpande, P. P., and Torchilin, V. P. (2012) Liposomes loaded with paclitaxel and modified with novel triphenylphosphonium-PEG-PE conjugate possess low toxicity, target mitochondria and demonstrate enhanced antitumor effects *in vitro* and *in vivo*. *J. Control*

*Release* **159,** 393–402
45. Elmore, S. (2007) Apoptosis: a review of programmed cell death. *Toxicol. Pathol.* **35,** 495–516
46. Riedl, S. J., and Salvesen, G. S. (2007) The apoptosome: signalling platform of cell death. *Nat. Rev. Mol. Cell Biol.* **8,** 405–413
47. Liu, J., Epand, R. F., Durrant, D., Grossman, D., Chi, N. W., Epand, R. M., and Lee, R. M. (2008) Role of phospholipid scramblase 3 in the regulation of tumor necrosis factor-α-induced apoptosis. *Biochemistry* **47,** 4518–4529
48. Lacombe, M. L., Tokarska-Schlattner, M., Epand, R. F., Boissan, M., Epand, R. M., and Schlattner, U. (2009) Interaction of NDPK-D with cardiolipin-containing membranes: structural basis and implications for mitochondrial physiology. *Biochimie* **91,** 779–783
49. Ji, J., Kline, A. E., Amoscato, A., Samhan-Arias, A. K., Sparvero, L. J., Tyurin, V. A., Tyurina, Y. Y., Fink, B., Manole, M. D., Puccio, A. M., Okonkwo, D. O., Cheng, J. P., Alexander, H., Clark, R. S., Kochanek, P. M., Wipf, P., Kagan, V. E., and Bayir, H. (2012) Lipidomics identifies cardiolipin oxidation as a mitochondrial target for redox therapy of brain injury. *Nat. Neurosci.* **15,** 1407–1413
50. Samhan-Arias, A. K., Ji, J., Demidova, O. M., Sparvero, L. J., Feng, W., Tyurin, V., Tyurina, Y. Y., Epperly, M. W., Shvedova, A. A., Greenberger, J. S., Bayir, H., Kagan, V. E., and Amoscato, A. A. (2012) Oxidized phospholipids as biomarkers of tissue and cell damage with a focus on cardiolipin. *Biochim. Biophys. Acta* **1818,** 2413–2423
51. Tyurina, Y. Y., Poloyac, S. M., Tyurin, V. A., Kapralov, A. A., Jiang, J., Anthonymuthu, T. S., Kapralova, V. I., Vikulina, A. S., Jung, M. Y., Epperly, M. W., Mohammadyani, D., Klein-Seetharaman, J., Jackson, T. C., Kochanek, P. M., Pitt, B. R., Greenberger, J. S., Vladimirov, Y. A., Bayir, H., and Kagan, V. E. (2014) A mitochondrial pathway for biosynthesis of lipid mediators. *Nat. Chem.* **6,** 542–552
52. Belikova, N. A., Vladimirov, Y. A., Osipov, A. N., Kapralov, A. A., Tyurin, V. A., Potapovich, M. V., Basova, L. V., Peterson, J., Kurnikov, I. V., and Kagan, V. E. (2006) Peroxidase activity and structural transitions of cytochrome c bound to cardiolipin-containing membranes. *Biochemistry* **45,** 4998–5009
53. Prasad, S., Maiti, N. C., Mazumdar, S., and Mitra, S. (2002) Reaction of hydrogen peroxide and peroxidase activity in carboxymethylated cytochrome *c*: spectroscopic and kinetic studies. *Biochim. Biophys. Acta* **1596,** 63–75
54. de Jongh, H. H., Ritsema, T., and Killian, J. A. (1995) Lipid specificity for membrane mediated partial unfolding of cytochrome *c*. *FEBS Lett.* **360,** 255–260
55. Chattopadhyay, K., and Mazumdar, S. (2003) Stabilization of partially folded states of cytochrome *c* in aqueous surfactant: effects of ionic and hydrophobic interactions. *Biochemistry* **42,** 14606–14613
56. Sanghera, N., and Pinheiro, T. J. (2000) Unfolding and refolding of cytochrome *c* driven by the interaction with lipid micelles. *Protein Sci.* **9,** 1194–1202
57. Dong, L. F., Low, P., Dyason, J. C., Wang, X. F., Prochazka, L., Witting, P. K., Freeman, R., Swettenham, E., Valis, K., Liu, J., Zobalova, R., Turanek, J., Spitz, D. R., Domann, F. E., Scheffler, I. E., Ralph, S. J., and Neuzil, J. (2008) α-Tocopheryl succinate induces apoptosis by targeting ubiquinone-binding sites in mitochondrial respiratory complex II. *Oncogene* **27,** 4324–4335
58. Shiau, C. W., Huang, J. W., Wang, D. S., Weng, J. R., Yang, C. C., Lin, C. H., Li, C., and Chen, C. S. (2006) α-Tocopheryl succinate induces apoptosis in prostate cancer cells in part through inhibition of Bcl-xL/Bcl-2 function. *J. Biol. Chem.* **281,** 11819–11825
59. Borisenko, G. G., Martin, I., Zhao, Q., Amoscato, A. A., Tyurina, Y. Y., and Kagan, V. E., (2004) Glutathione propagates oxidative stress triggered by myeloperoxidase in HL-60 cells: evidence for glutathionyl radical-induced peroxidation of phospholipids and cytotoxicity. *J. Biol. Chem.* **279,** 23453–23462
60. Davies, M. J. (2011) Myeloperoxidase-derived oxidation: mechanisms of biological damage and its prevention. *J. Clin. Biochem. Nutr.* **48,** 8–19
61. Rezk, B. M., van der Vijgh, W. J., Bast, A., and Haenen, G. R. (2007) α-Tocopheryl phosphate is a novel apoptotic agent. *Front. Biosci.* **12,** 2013–2019
62. Nishio, K., Ishida, N., Saito, Y., Ogawa-Akazawa, Y., Shichiri, M., Yoshida, Y., Hagihara, Y., Noguchi, N., Chirico, J., Atkinson, J., and Niki, E. (2011) α-Tocopheryl phosphate: uptake, hydrolysis, and antioxidant action in cultured cells and mouse. *Free Radic. Biol. Med.* **50,** 1794–1800
63. Munteanu, A., Zingg, J. M., Ogru, E., Libinaki, R., Gianello, R., West, S., Negis, Y., and Azzi, A. (2004) Modulation of cell proliferation and gene expression by α-tocopheryl phosphates: relevance to atherosclerosis and inflammation. *Biochem. Biophys. Res. Commun.* **318,** 311–316
64. Gianello, R., Hall, W. C., Kennepohl, E., Libinaki, R., and Ogru, E. (2007) Subchronic oral toxicity study of mixed tocopheryl phosphates in rats. *Int. J. Toxicol.* **26,** 475–490
65. Neuzil, J., Tomasetti, M., Zhao, Y., Dong, L. F., Birringer, M., Wang, X. F., Low, P., Wu, K., Salvatore, B. A., Ralph, S. J. (2007) Vitamin E analogues, a novel group of "mitocans," as anticancer agents: the importance of being redox-silent. *Mol. Pharmacol.* **71,** 1185–1199
66. Rodríguez-Enríquez, S., Hernández-Esquivel, L., Marín-Hernández, A., Dong, L. F., Akporiaye, E. T., Neuzil, J., Ralph, S. J., Moreno-Sánchez, R. (2012) Molecular mechanism for the selective impairment of cancer mitochondrial function by a mitochondrially targeted vitamin E analogue. *Biochim. Biophys. Acta* **1817,** 1597–1607
67. Liewald, F., Demmel, N., Wirsching, R., Kahle, H., Valet, G. (1990) Intracellular pH, esterase activity, and DNA measurements of human lung carcinomas by flow cytometry. *Cytometry* **11,** 341–348

Metabolism:

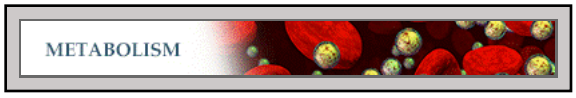


# Structural Re-arrangement and Peroxidase Activation of Cytochrome *c* by Anionic Analogues of Vitamin E, Tocopherol Succinate and Tocopherol Phosphate

Naveena Yanamala, Alexander A. Kapralov, Mirjana Djukic, Jim Peterson, Gaowei Mao, Judith Klein-Seetharaman, Detcho A. Stoyanovsky, Jan Stursa, Jiri Neuzil and Valerian E. Kagan

*J. Biol. Chem. 2014, 289:32488-32498.*
*doi: 10.1074/jbc.M114.601377 originally published online October 2, 2014*